How are anatomical and hydraulic features of the mangroves Avicennia marina and Rhizophora mucronata influenced by siltation?

Article *in* Trees · January 2016

DOI: 10.1007/s00468-016-1357-x

CITATIONS
2

READS
206

5 authors, including:

Hannes De Deurwaerder
Ghent University
11 PUBLICATIONS **70** CITATIONS
SEE PROFILE

Judith Okello
Kenya Marine and Fisheries Research Institute (KMFRI)
8 PUBLICATIONS **50** CITATIONS
SEE PROFILE

Nico Koedam
Vrije Universiteit Brussel
272 PUBLICATIONS **9,335** CITATIONS
SEE PROFILE

Nele Schmitz
Thünen Institute
57 PUBLICATIONS **606** CITATIONS
SEE PROFILE

Trees (2016) 30:35–45
DOI 10.1007/s00468-016-1357-x

ORIGINAL ARTICLE

How are anatomical and hydraulic features of the mangroves *Avicennia marina* and *Rhizophora mucronata* influenced by siltation?

Hannes De Deurwaerder[1] · J. A. Okello[2,3] · N. Koedam[3] · N. Schmitz[3,4] · K. Steppe[1]

Received: 16 February 2015 / Accepted: 16 January 2016 / Published online: 29 January 2016

Abstract

Key message **This article provides significant data in the debate on whether siltation might have a negative impact on the hydraulic functioning of two widespread mangrove tree species *Avicennia marina* and *Rhizophora mucronata*.**

Abstract Elevated sediment addition, or siltation, within mangrove ecosystems is considered as being negative for trees and saplings, resulting in stress and higher mortality rates. However, little is known about how siltation influences the hydraulic functioning of mangrove trees. Comparing two mangrove tree species (*Avicennia marina* Vierh. Forsk. and *Rhizophora mucronata* Lam.) from low and high-siltation plots led to the detection of anatomical and morphological differences and tendencies. Adaptations to high siltation were found to be either mutual among both species, e.g., significant smaller single leaf area ($p_{A.marina} = 0.058$, $F1.38 = 3.8$; $p_{R.mucronata} = 0.005$, $F1.38 = 8.7$; $n = 20 \times 20$) and a tendency towards smaller stomatal areas ($p_{A.marina} = 0.131$, $F1.8 = 2.8$; $p_{R.mucronata} = 0.185$, $F1.8 = 2.1$, $n = 5 \times 60$), or species-specific trends for *A. marina*, such as higher phloem band/growth layer ratios ($p = 0.101$, $F1.8 = 3.4$, $n = 5 \times 3$) and stomatal density ($p = 0.052$, $F1.8 = 5.2$, $n = 5 \times 4$). All adaptations seemingly contributed to a comparable hydraulic conductivity independent of the degree of siltation. These findings indicate that silted trees level off fluctuations in their hydraulic performance as a survival mechanism to cope with this less favourable environment. Most of the trees' structural adaptations to cope with siltation are similar to known drought stress-imposed adaptations.

Keywords Hydraulic conductivity · Wood anatomy · Stomata · Leaf area · Phloem band/growth layer ratio

Communicated by R. Reef.

N. Schmitz and K. Steppe contributed equally to this work.

✉ Hannes De Deurwaerder
hannes.dedeurwaerder@ugent.be

K. Steppe
kathy.steppe@UGent.be

[1] Laboratory of Plant Ecology, Faculty of Bioscience Engineering, Ghent University (UGent), Coupure links 653, 9000 Ghent, Belgium

[2] Kenya Marine and Fisheries Research Institute (KMFRI), Headquarter and Mombasa Station, P.O. Box 81651 080100, Mombasa, Kenya

[3] Laboratory of Plant Biology and Nature Management (APNA), Vrije Universiteit Brussel (VUB), Pleinlaan 2, 1050 Brussels, Belgium

[4] Universität für Bodenkultur Wien (BOKU), Gregor-Mendel-Straße 33, 1180 Vienna, Austria

Introduction

Mangrove forests consist of tropical trees and shrubs growing at the interface between sea and land. This intertidal zone forms a highly productive and ecologically important ecosystem, often found in combination with coral reefs and seagrass beds (Kathiresan and Bingham 2001; Tomlinson 1986). With the exception of the most exposed or rockiest shorelines, mangrove forests occupy all regions between mean sea level and the highest spring tide in tropical and subtropical latitudes. These forests are hence regularly exposed to water level fluctuations, resulting in varying degrees of hypoxia and changes in soil

water salt concentration (Alongi 2008). Mangrove trees can grow and function well at salinities up to 90 parts per thousand (ppt = g L^{-1}) (Robert et al. 2009), but they perform at best when salinity fluctuates between 5 and 75 ppt (Krauss et al. 2008). This extremely saline environment claims a low water potential (<−2.5 MPa), making water absorption through the roots and ascent to the leaves a challenge (Scholander et al. 1964).

Research worldwide points towards siltation, defined as an unusually high increase in sedimentation rate, as one of the direct causes for the loss of mangrove trees (Ellison 1998; Gordon 1987; Lugo and Cintron 1975; Terrados et al. 1997; van Mensvoort 1998). Both natural processes, such as hurricanes (Castañeda-Moya et al. 2010), storm surges and tsunamis, and anthropogenic processes, such as waste discharges of shrimp ponds (Vaiphasa et al. 2007), river dredging or sediment runoff and erosion due to land use changes, can result in silted mangrove areas. Moreover, when siltation rates exceed 1 cm $year^{-1}$, they might cause a serious dieback and high death ratio within the mangrove forest (Ellison 1998). This statement results from the review by Ellison (1998), where the various included studies indicate the negative impact of siltation. Among other studies, Vaiphasa et al. (2007) noticed a significant lower diameter growth at breast height (DBH) and height growth for mature *A. marina* and *Lumnitzera racemosa* mangrove trees [about 17.6 % (DBH), 7.8 % (height) and 11.7 % (DBH), 5.7 % (height), respectively], and a total absence of colonisation by seedlings within study sites that were silted with discharge of shrimp ponds (>5 cm $year^{-1}$). Other observations indicated the loss of 100 ha of mangrove ecosystems by the deposit of dredged-up sediment originating from the Mokowe Sea Jet construction in Kenya (Abuodha and Kairo 2001).

Knowledge on what causes the negative effects of siltation on mangrove trees is still incomplete. However, Ellison (1998) hypothesises that the decreased mangrove viability is the result of sediment particles smothering the aerial roots. This results in a decreased oxygen ventilation of the roots causing lowered radial oxygen loss. The latter process is vital for the development of an aerobic protective rhizosphere around the root surface and to oxidise toxic products before they are taken up by the plant (Pi et al. 2009). Moreover, this inhibition of gas exchange between the atmosphere and the roots results in root damage and oxygen deficiency (Abuodha and Kairo 2001; Ellison 1998), with potential strong dieback of root tips (McKee 1996). Subsequently, this hypothesised phenomenon might lead to a decreased ability of the root system in the uptake of water and nutrients from the soil.

The aim of this study was to verify whether siltation has a negative effect on the hydraulic functioning of *A. marina* and *R. mucronata* in the mangrove forest of Mikindani, Mombasa (Kenya), and when it does, how this impacts the tree's hydraulic performance. We hypothesise that siltation may cause responses that, considering the root smothering hypothesis, might be very similar to drought stress-induced responses conform the study of Ball (1988), where water-logged soils, without efficient oxygen supply, hinder water uptake by mangrove roots. We put forward that siltation may, therefore, lead to changes in leaf characteristics, hydraulic conductivity and wood anatomical properties, which are expected to be in line with common drought responses found in trees and plants. Therefore, our specific working hypotheses were: (1) trees in high-siltation sites will have smaller leaves; (2) hydraulic conductivity will be lower in high-siltation sites; and (3) trees in high-siltation sites will have smaller xylem vessels, and a higher phloem band/growth layer ratio. We compared *A. marina* and *R. mucronata* because they are worldwide the most characteristic determinants of mangrove formations and have a very wide geographical range (Quisthoudt et al. 2013). Additionally, since the type of aerial roots is very different between both species, pencil roots in case of *A. marina* and prop roots in case of *R. mucronata*, the impact of siltation is expected to be different.

Materials and methods

Study area

The study area is located at 4°00′S 39°38′E in the mangrove forest of Mikindani, Tudor Creek, in the suburbs of Mombasa, Kenya (Fig. 1). Tudor Creek is due to its open access to the ocean subjected to maximal tidal ranges of approximately 4 m (Brakel 1982). Human encroachment (land use change increased from 5.9 ha in 1969 to over 50 ha in 1992) on the slopes flanking the mangroves resulted in siltation of the local mangrove vegetation (Mohamed et al. 2009). The

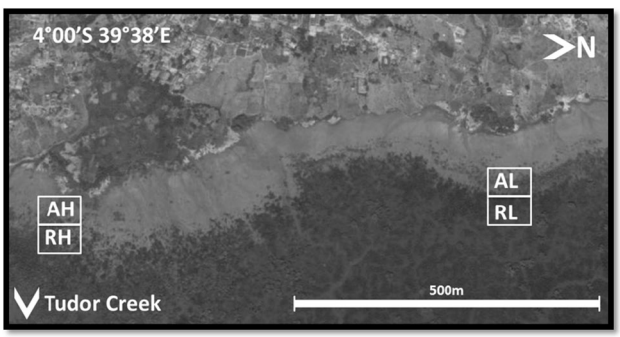

Fig. 1 Schematic overview of the study area showing both a high (H) and a low (L) siltation site, each subdivided conform species, i.e. *A. marina* (A) and *R. mucronata* (R)

steep slopes are increasingly turned into plots for both houses and crop fields. In addition, huge amounts of marine sands were brought into this forest by storm surges originating from the heavy rains in 1997 caused by the El Niño Southern Oscillation and resulting in silted subsoil. Besides siltation, the squatter suburbs in Mikindani also cause influx of domestic wastewater.

Mombasa and the surrounding regions are subjected to a warm and tropical climate with two rainy and two dry seasons a year. The wettest period occurs during April and May, while the second, less pronounced, rainy period takes place in October and November. The total annual rainfall is around 1144 mm $year^{-1}$ and the annual temperature reaches an average of 26.4 °C (Lieth et al. 1999).

The study area was divided into four measurement plots based on difference in siltation and dominant mangrove tree species (Fig. 1). Two low (L) and two high (H) siltation sites were defined, with the two studied species, *A. marina* (A) and *R. mucronata* (R) represented at each siltation level. These levels were gauged by soil sampling, colour of the soil, steepness of the hill slope and the shortest distance to the Creek. The plots were chosen in close proximity to each other to ensure that all other conditions except siltation were similar. The high-siltation plots had a yellow–brown coloured upper soil layer ($\sim$10 cm) with a loamy to sandy texture, which bore some similarity with those of the adjacent slopes, while the upper soil layer of the low-siltation plots was dark and muddy. Steep hill slopes increase the chance of land erosion (low-siltation site approx. 5.4°; high-siltation site approx. 8.7°), while distance to the Tudor Creek river bay would increase substrate deposited by river overflows or storm surges (Furukawa et al. 1997).

All sites were located in inundation class IV, which indicates flooding by seawater (35 ppt) twice a day (according to the oceanic tides) (Krauss et al. 2008). Fresh water input mostly originated from rainfall and run-off. The measurement campaign took place from 10 July to 15 August 2011 [DOY (day of year) 201, 202, 204, 206, 208, 209, 210, 213, 215 and 216].

Soil characteristics

To estimate natural soil variability and to confirm the suitability of locations selected for measurements within the study site, six soil cores (60 cm in depth) were randomly taken per site. Three samples were taken during spring tide and three more during neap tide with a depth stratification of 0–2, 2–4, 4–6, 6–9, 9–15, 15–20 cm. Measurements of nutrient content (μM), density (g m^{-3}), water content (%), porosity and grain size (μm) were performed using standard protocols. In the field, salinity (ppt), pH, dissolved oxygen (mg L^{-1}) (both measured using a Professional plus Multi-Parameter instrument, YSI Inc, Ohio, USA), colour and width of these soil layers were measured or estimated.

In the lab, nutrients were extracted from weighed samples ($\sim$10 g dry weight) by adding 40 ml of 1 N KCl. After shaking the solution for at least 1 h, centrifugation was applied. Nutrients in the obtained supernatant were analysed according to the methods described by Parson et al. (1984) and APHA (1998). Orthophosphate ($PO_4^3 - P$) was determined with a UV vis spectrophotometer using the ascorbic acid method at 885 nm. Ammonia (NH_4^+) was determined using the indophenol method with a spectrophotometric read out at 630 nm following a minimum of 6 h solution developing in the dark. Dissolved nitrate and nitrite (NO_3^- and NO_2^-) were determined using the cadmium reduction method and measured colorimetrically at 543 nm (GENESYS 10S double beam UV–VIS spectrophotometer, Thermo Electron Scientific Instruments LLC, Madison, USA). Analytical quality check was carried out by running procedural blanks alongside the samples as well as through the use of standards. All chemicals used for analysis were of analytical grade and all the glassware was pre-washed with water and phosphate free detergent, rinsed with tap water, soaked in 5 % hydrochloric acid overnight and subsequently rinsed again using deionized water.

Sample selection

Ten mature trees of approximately the same height and stem circumference, free from grazing and cutting damage, were selected for each species per site. Stem diameter at 30 cm above the highest prop root (D30) or 130 cm above ground level (D130) was measured for *R. mucronata* and *A. marina*, respectively. Branches sampled for hydraulic and anatomical measurements had a diameter of 10 mm, a straight habitus and as few nodes as possible. Branches were at equal height above ground level and were fully exposed to solar radiation.

Leaf characteristics

Stomatal imprints of five *R. mucronata* leaves, subsampled over four replicates per stomatal peel, were collected using the clear nail varnish method. Due to the hairy habitus and the sunken stomata of *A. marina* leaves, the maceration technique was applied (Carr 2000). The abaxial epidermis layer was removed by bathing the leaves in a 5:1 mixture of hydrogen peroxide and glacial acetic acid for 10 h at 65 °C. Subsequently, the epidermis was stained with alcian blue-safranin and mounted on a microscope slide using glycerine jelly. The 5 macerated leaf fragments were subsampled over four microscopic fields of view ($n = 5 \times 4$),

which were photographed (Colorview IIIv soft imaging system $0.63 \times 1/2'' = 11.5$; $2/3 = 17.5$, Olympus) and analysed with the software Cell-D (Olympus Europe, Digital Image Systems, Athens, Greece). For both *R. mucronata* and *A. marina*, the number of stomata as well as the width and length of 15 randomly picked stomata openings was measured per field of view. These data were further used to calculate stomatal density (#mm^{-2}), stomatal area (μm^2) and the pore area index, i.e., the total stomatal pore area per unit leaf area.

The number of leaves per branch of 20 distinct trees per plot was determined and leaf area of each individual leaf was measured with a Portable Laser Leaf Area Meter (CI-202L, CID Bio-Sciences Inc., Washington, USA), which was used to calculate the average leaf size and the total leaf area per branch.

Branch hydraulic conductivity and anatomy

To test potential changes in the hydraulic conductivity due to siltation, for a randomly selected tree, two branches with an approximate diameter of 10 mm were sampled per plot (AH, AL, RH, RL) per measurement day. The first branch was cut in the morning (a.m., between 9:30 and 11:00 a.m.) while the second one was cut in the afternoon (p.m., between 1:30 and 3:00 p.m.). Since this protocol has been performed on 10 different days, the total sample size was 20 branches per plot resulting from 10 different trees. All branches were cut under water to avoid cavitation (Hao et al. 2009). Sampled branches of *A. marina* were on average 130 cm in length, while those of *R. mucronata* were on average 60 cm.

Branch hydraulic conductivity (Angeles et al. 2002; López-Portillo et al. 2005) was measured using a set-up as described in Sperry et al. (1988) and Choat et al. (2011). Branch segments of approximately 10 mm in diameter and 10 cm in length were placed within the set-up, with the proximal end connected to the tubing system coming from a reservoir containing a solution of filtered seawater (1 %) and distilled water. This solution is similar to the ionic concentration of the sap within a mangrove tree (Ball 1988; Choat et al. 2011; Stuart et al. 2007). The distal end of the branch was connected to a calibrated pipette (0.1 mm) loaded with dye and positioned on graph paper graded to 1 mm. By taking sequential photographs of the moving dye in the pipette, every 30 s within a time span of 5 min (Canon, Eos D1000), we were able to measure the flow velocity of the dye using the ImageJ software (Ounis et al. 2005). Knowing the volume and the length of the pipette we could calculate the sap flow rate (F) (m^3 s^{-1}) through the branch. Applied pressure (Ψ) (Pa) on the branch is calculated as shown in Eq. 1:

$$\Psi = h \times \rho \times g \tag{1}$$

where (ρ) (kg m^{-3}) is the density of the fluid, g (m s^{-2}) is the acceleration due to gravity, and h (m) is the height of the perfusion solution reservoir with respect to the branch. Specific conductivity (K_s) (kg m^{-1} s^{-1} MPa^{-1}) was calculated using Eq. 2 (López-Portillo et al. 2005):

$$K_s = \frac{F \times \rho}{\Psi} \times \frac{1}{S_x} \times L_{branch} \tag{2}$$

where S_x is the respective xylem cross-sectional area of the branch segment (m^2) and L_{branch} (m) is the length of the branch segment.

Before and after the experiment, all examined branch segments were weighed, using the weight difference as an indication of water uptake or loss by the branch during the experiment. Subsequently, a 5 cm long segment of the examined branch was cut, placed perpendicular on the graph paper with the aim to photograph the transverse section on which bark area (S_b), xylem area (S_x) and pith area (S_p) could be measured, followed by labelling and placement in preservation mixture (70 % ethanol and some drops of glycerol) for anatomical analysis.

Anatomical transverse micro-sections (25 μm) for five branch parts per plot were made with a sledge microtome (GSL 1, MICROT L, Gärtner & Schweingruber, Zürich, Switzerland) (Gartner and Nievergelt 2010). These sections were stained with a safranin and alcian blue mixture. Subsequently, for every wood slide, three microscopic fields of view have been photographed (Colorview IIIv soft imaging system $0.63 \times 1/2'' = 11.5$; $2/3 = 17.5$, Olympus). Further analysis was performed with the software Cell-D (Olympus Europe, Digital Image Systems, Athens, Greece).

All vessels within a given field of view ($n = 5 \times 3$) were counted and width (a) (μm) and length (b) (μm) of lumens of 40 randomly selected vessels were measured (Fig. 2). From these measurements, vessel area (A_{vessel}) (μm^2) (Eq. 3), vessel number and conductive area per cross-sectional area ($A_{conductive}$) (Eq. 4) were calculated. For *A. marina*, having a wood anatomy characterised by successive cambia (Schmitz et al. 2007, 2008) also phloem band/growth layer ratio (%) was calculated by dividing the phloem band (μm^2) (area 1, Fig. 2, b1) by the area of the growth band (μm^2) (area 2, Fig. 2, b2). The phloem band is designated as a zone of phloem strands united in a band of parenchyma tissue, bordered by a layer of sclereids on the outer side (Schmitz et al. 2008), whilst the growth layer designates one ontogenetic unit of both xylem and phloem (Schmitz et al. 2008).

$$A_{vessel} = \pi \times \frac{a}{2} \times \frac{b}{2} \tag{3}$$

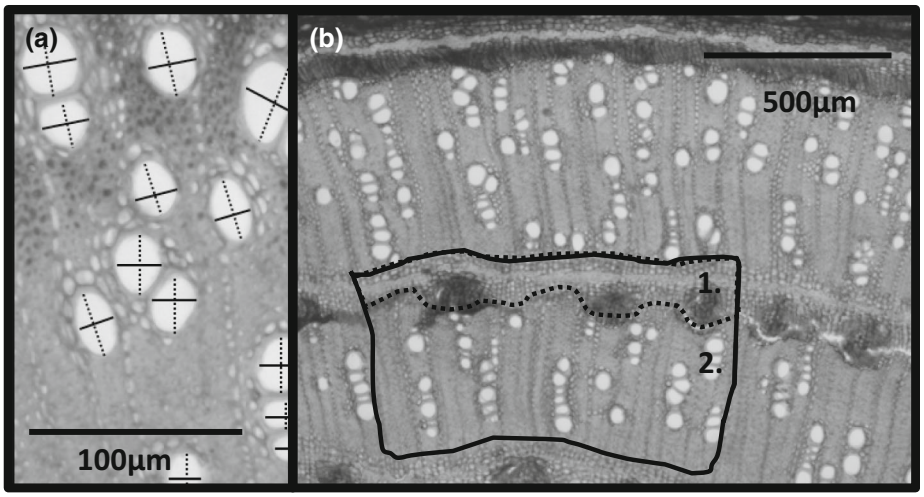

Fig. 2 Anatomical transverse branch section: **a** vessel length (*dotted*) and vessel width (*full*); and **b** measurements required for phloem band/growth band ratio calculations on *A. marina*: (*1*) *dotted frame* indicates area of phloem tissue. (*2*) *Full frame* indicates the total growth layer

$$A_{\text{conductive}} = \frac{A_{\text{vessel}} \times \text{Vessel number}}{A_{\text{branch}}} \quad (4)$$

with A_{branch} the respective cross-sectional area of the branch (μm^2).

Statistical data analysis

All statistical analyses were performed using RStudio (Boston, MA, USA). The datasets of selected trees characteristics, the total leaf area, number of leaves per branch and the specific conductivity (K_s) were suited for a non-parametric Mann–Whitney *U* test (MWU), comparing non-normal distributed *A. marina* and *R. mucronata* between two distinct sites, differing in degree of siltation. For all other data, a Nested ANOVA approach was used. Power Analysis ($1 - \beta = 0.8$) was performed to estimate desired sample size in support of describing some moderate effects not being detected due to the rather small study sample sizes. This analysis allows evaluating the sample size being large enough to properly detect a biological significant effect, given the observed level of variation (Thomas 1997). Where low, non-significant p values are accompanied by relative small sample size estimations, effects of siltation observed in the data might, thus, be plausible despite non-significant results. These cases will be denoted by the use of the term 'tendency'. The power analysis is not used as a single argument, but is combined with ratifications from existing literature.

Results

General site characteristics

None of the measured tree characteristics, including tree diameter at D_{130} or D_{30} (cm), three height (m), height of branch cutting (cm) and number of branches per tree, significantly differed ($p > 0.05$) when comparing the four measurement sites (Table 1). There was a higher sand fraction and higher number of contrasting soil layers in the high-siltation sites. Similar trends were observed for the amount of dissolved oxygen and the redox potential in the upper 10 cm thick soil layer. Slightly lower salinity levels were noted in the high-siltation than in the low-siltation sites. When comparing the upper 10 cm thick soil layer, the highest levels of nutrients (phosphates, nitrates and ammonia) were found in the low-siltation sites. Below this 10 cm thick soil layer, the highest amounts of nutrients were found in the high-siltation sites.

Leaf characteristics

Rhizophora mucronata trees subjected to high-siltation had a significantly ($p = 0.005$, $F1.38 = 8.7$) smaller single leaf area (cm^2) and significant less leaves per branch ($p = 0.046$, MWU) as compared to low-siltation trees (Table 2). Similarly, *A. mucronata* displayed significant less leaves per branch ($p = 0.031$, MWU) and the tendency of developing smaller single leaf area (cm^2) ($p = 0.058$, $F1.38 = 3.8$) when subjected to high degrees of siltation. Moreover, the observations indicated that the branches of trees on silted substrate seemingly had more and smaller leaves per branch for both tree species. This alteration resulted in the tendency of increased total leaf area (cm^2) ($p = 0.064$, MWU) for *A. marina* in high-siltation plots whereas for *R. mucronata* no difference was found ($p = 0.685$, MWU) between low- and high-siltation plots.

When sampled leaves originated from trees in high-siltation sites, stomatal density for *A. marina* tended toward higher values ($p = 0.052$, $F1.8 = 5.2$) (Table 2), while a tendency for lowered stomatal area was noticed for

Table 1 Biotic and abiotic characteristics of the plots and the sampled *A. marina* (A) and *R. mucronata* (R) trees located within the high- (H) and low- (L) siltation sites

	Low siltation		High siltation		*n*
	A	R	A	R	
Micro-climate					
RH (a.m.) (%)	68 (66/70)	67 (64/68)	67 (65/69)	66 (64/71)	10
RH (p.m.) (%)	61 (58/62)	62 (60/67)	61 (59/65)	62 (60/63)	10
T (a.m.) (°C)	28.6 (28.2/29.9)	29.3 (28.4/29.8)	28.9 (28.4/29.6)	28.7 (28.1/29.6)	10
T (p.m.) (°C)	31.0 (30.2/32.0)	30.7 (29.3/31.8)	30.6 (29.6/31.9)	31.0 (30.1/31.7)	10
Tree characteristics					
D_{30}/D_{130} (cm)	11.20 (4.10/14.39)	11.68 (8.20/17.45)	10.59 (9.40/11.97)	8.27 (7.43/12.17)	10
Tree height (m)	3.10 (2.97/3.20)	2.19 (2.09/2.56)	2.90 (2.85/3.01)	2.31 (2.22/2.38)	10
h_{branch} (cm)	132 (117/156)	122 (116/139)	131 (113/143)	113 (100/123)	19–20
No. of branches/tree	36 (25/39)	20 (18/22)	36 (30/43)	27 (24/29)	19–20
Soil analysis					
Sand fraction (%)	53.2	61.3	65.9	63.9	
No. of distinct soil layers	3	3	4	4	
DO in upper 10 cm (mg L^{-1})	3.1	3.2	5.7	5.4	
Soil water salinity (ppt)	55.0	49.5	53.0	48.0	
Redox potential	−43.0	−65.8	−14.5	−55.0	

Medians of this random survey are given with the 25 and 75 % percentile between brackets. The number of decimals is conforming to the precision of the measuring equipment. The number *n* indicates measurements per plot. Redox potential and soil water salinity are given for the upper 10 cm soil layer

RH relative humidity, (a.m.) and (p.m.) are measures during the morning (between 9:30 and 11:00 a.m.) and in the afternoon (between 1:30 and 3:00 p.m.), respectively, *T* temperature, *D30/D130* stem circumference at 30 cm above the highest prop root or 130 cm above ground level for *R. mucronata* and *A. marina*, respectively, h_{branch} height of branch cutting for hydraulic conductivity measurements, *DO* dissolved oxygen

both species (Table 2) ($p_{\text{Avicennia}} = 0.131$, $F1.8 = 2.80$; $p_{\text{Rhizophora}} = 0.185$, $F1.8 = 2.1$). *A. marina* sampled in the high-siltation site showed a tendency ($p = 0.080$, $F1.8 = 40$) to higher pore area index in comparison to those sampled in low-siltation sites, a trend which was, however, absent in *R. mucronata* ($p = 0.713$, $F1.8 = 0.15$).

Branch hydraulic conductivity and anatomy

There were no statistical differences in branch K_s when comparing high- and low-siltation sites for both species (Table 2). Also notable were the back-flows, where the dye moved against the imposed pressure direction. This phenomenon occurred more within branches of silted trees (Fig. 3). Especially, branches from silted *R. mucronata* trees sampled in the morning were most prone to this opposite flow direction.

There were no differences ($p > 0.05$, MWU) observed in tissue proportions (percentages of bark, xylem or pith area) of branches of trees of a given species occurring in the high- and low-siltation plots (Fig. 4). However, when comparing both species, strong differences existed in their tissue distribution. On average, half of the total cross-sectional area of a *R. mucronata* branch is bark, which consists of a very high proportion of aerenchyma (Okello et al. 2014). Most of the remaining area, which is on average 35 % of the total cross-sectional area, is xylem, leaving 15 % for pith area. In *A. marina* branches 80 % of the total cross-sectional area consisted of xylem, whilst bark accounted for 15 % and pith for 5 %.

High- or low-siltation did not result in a significant difference in vessel density, vessel area or conductive area per cross-sectional area for both examined species (Table 2). *A. marina* showed a tendency towards a higher phloem band/growth layer ratio ($p = 0.101$, $F1.8 = 3.4$,) when grown in the high-siltation site (Table 2).

Discussion

Common adaptations of mangrove tree species to siltation

The additional 10 cm thick layer and higher fraction of sand in the high-siltation site indicate that more marine sediments settled in this site during the storm surges of 1997. This smothered the active tissues of the aerial roots. As a result, *A. marina* and *R. mucronata* trees growing in high-siltation sites had more, but smaller leaves. Siltation may have induced oxygen deficiency at

Table 2 Leaf morphology (Leaf), branch specific conductivity (K_s) (kg m^{-1} s^{-1} MPa^{-1}), vessel and stomata characteristics (resp. Vessel and Stomata) of the sampled *A. marina* and *R. mucronata* trees located within the high (H) and low (L) siltation sites

	Avicennia marina					*Rhizophora mucronata*					*n*
	L	H	*F* test	*p* value	Power ($1 - \beta = 0.80$)	L	H	*F* test	*p* value	Power ($1 - \beta = 0.80$)	
Leaf											
Single leaf area (cm^2)	11.42 (8.58/13.86)	9.56 (7.55/11.43)	$F1.38 = 3.8$	0.058	82 ($\Delta = 2$)	46.15 (37.79/56.30)	37.25 (30.76/47.08)	$F1.38 = 8.7$	0.005**	57 ($\Delta = 8$)	20 × 20
Total leaf area (cm^2)	1803.3 (1561.7/2188.5)	1899.8 (1477.2/2387.7)	–	0.064	–	1743.9 (1400.2/2470.9)	1910.5 (1442.0/2131.4)	–	0. 685	–	20
No. of leaves/branch (#)	237 (197/263)	268 (219/317)	–	0.031*	–	43 (34/56)	64 (45/73)	–	0.046*	–	14
K_s											
K_s a.m. (kg m^{-1} s^{-1} MPa^{-1})	0.034 (0.011/0.046)	0.026 (0.013/0.032)	–	0.597	–	0.050 (0.022/0.108)	0.013 (−0.013/0.118)	–	0.326	–	10
K_s p.m. (kg m^{-1} s^{-1} MPa^{-1})	0.028 (0.014/0.037)	0.023 (0.018/0.043)	–	0.940	–	0.081 (0.042/0.260)	0.041 (0.028/0.53)	–	0.082	–	10
Vessel											
Vessel density (# vessels/mm^2)	61.1 (56.3/77.8)	59.5 (56.9/68.7)	$F1.8 = 0.00$	0.980	20974 ($\Delta = 0.3$)	56.4 (43.6/65.7)	59.2 (48.9/87.4)	$F1.8 = 0.10$	0.460	52 ($\Delta = 12$)	5 × 3
Vessel lumen area (μm^2)	1124.1 (849.5/1374.1)	915.9 (867.6/1276.1)	$F1.8 = 1.0$	0.346	1432($\Delta = 131$)	2156.5 (1905.5/2294.4)	2087.7 (1471.7/2428.4)	$F1.8 = 0.2$	0.704	2464 ($\Delta = 112$)	5 × 120
Total lumen area ($\times 10^{-3}$) (mm^2 vessel/mm^2 branch area)	62.7 (58.1/80.4)	63.3 (57.7/76.9)	$F1.8 = 0.10$	0.763	421 ($\Delta = 56$)	118.8 (104.7/124.5)	127.3 (112.4/142.2)	$F1.8 = 0.16$	0.704	156 ($\Delta = 113$)	5 × 3
Phloem band/growth layer ratio (%)[a]	29.6 (28.2/32.9)	34.0 (31.5/25.7)	$F1.8 = 3.4$	0.101	21 ($\Delta = 4$)	–	–	–	–	–	5 × 3
Stomata											
Stomatal density (#/mm^2)	221.5 (205.2/250.0)	278.5 (250.5/294.4)	$F1.8 = 5.2$	0.052	7 ($\Delta = 44$)	120.5 (107.5/132.5)	122.8 (114.9/134.7)	$F1.8 = 0.18$	0.683	97 ($\Delta = 4$)	5 × 4
Stomatal area (μm^2)	305.8 (276.9/342.5)	280.3 (247.7/318.3)	$F1.8 = 2.8$	0.131	21 ($\Delta = 60$)	665.8 (588.1/739.5)	630.1 (558.0/695.4)	$F1.8 = 2.1$	0.185	165 ($\Delta = 43$)	5 × 60
Pore area index ($\times 10^{-3}$) (mm^2 stomata/mm^2 leaf area)	69.8 (65.1/77.1)	77.5 (73.5/79.5)	$F1.8 = 4.0$	0.080	29 ($\Delta = 0.006$)	79.9 (70.8/90.9)	76.4 (71.3/80.7)	$F1.8 = 0.15$	0.713	180 ($\Delta = 0.0025$)	5 × 4

Medians of this random survey are given with their 25 and 75 % percentile between brackets. For branch specific conductivity (K_s), a.m. and p.m. indicate the time period when branches were cut, respectively, in the morning (between 9:30 and 11:00 a.m.) and in the afternoon (between 1:00 and 3:00 p.m.). *p* level indicates the statistical significance level reached. *F* test results show the degrees of freedom of, respectively, the independent and dependent variable and the *F* value. *n* is the number of measurements per study site. Δ provides the delta difference value applied in the power calculation

[a] *A. marina* has concentric included phloem bands

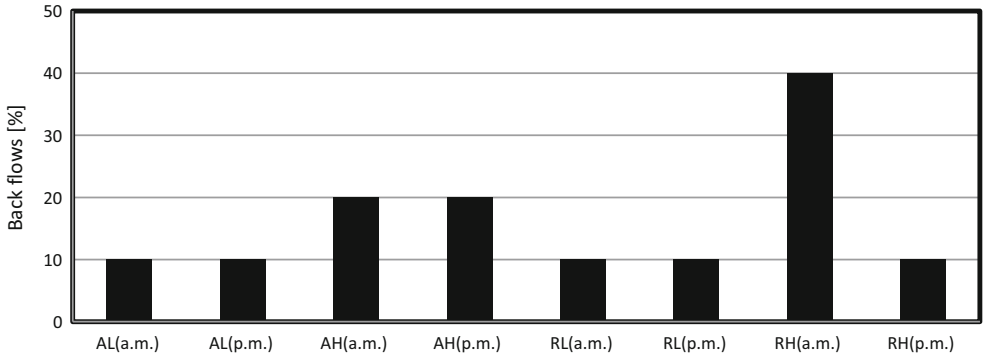

Fig. 3 Percentage of tested branches in which back-flow of the loading dye occurred. AL, AH, RL and RH represent *A. marina* in low-siltation, *A. marina* in high-siltation, *R. mucronata* in low-siltation and *R. mucronata* in high-siltation sites, respectively. (a.m.) sampling in the morning; (p.m.) sampling in the afternoon. $n_{(\text{branches/plot})} = 10$

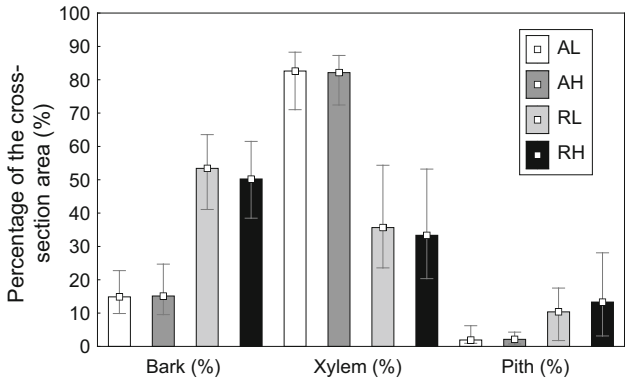

Fig. 4 Tissue distribution measured on cross sections of *A. marina* (A) and *R. mucronata* (R) branches from high (H) and low (L) siltation sites. *Plotted data* are medians with minimum and maximum values, $n = 20$

root level, and physiological drought stress has been shown to lead to a change in leaf size and number (Anyia and Herzog 2004; Burghardt et al. 2008; Heckenberger et al. 1998; Schurr et al. 2000). Smaller leaves enhance heat transfer rate, resulting in less transpiration and thus less water loss (Ball 1988; Brugnoli and Lauteri 1991; Quarrie and Jones 1977). In addition, a higher amount of small leaves is favourable when environmental conditions are too demanding and leaf shedding is induced, as discusses by Gu et al. (2007) on four birch genotypes. Besides smaller leaves, a tendency towards lowered stomatal area was found for both *A. marina* and *R. mucronata* in the sites with a higher degree of siltation. The presence of smaller stomata results in an advantage for trees handling drought stress (Franks and Beerling 2009; Franks et al. 2009; Franks and Farquhar 2001; Naz et al. 2010), since they have a faster response time, lose less water and have better water-use efficiencies (Franks and Beerling 2009). This fast closure reflex of the stomata is related to the smaller guard cells that can change osmotic and turgor pressure more quickly (Franks et al. 2009).

Trees subjected to siltation stress apparently adapted their leaf and stomatal anatomy but not their hydraulic conductivity. It seems that both tree species adapted anatomically and morphologically, thus ensuring a constant hydraulic conductivity independent of the soil siltation degree. However, we obtained K_s values one or two orders of magnitude lower than those previously reported by Lovelock et al. (2006) [0.131 ± 0.016 kg m^{-1} s^{-1} MPa^{-1} (Dwarf) and 0.190 ± 0.033 kg m^{-1} s^{-1} MPa^{-1} (Fringe) both for *Rhizophora mangle*] and McClenahan et al. (2004) [0.68 ± 0.09 kg m^{-1} s^{-1} MPa^{-1} (winter) and 3.65 ± 0.80 kg m^{-1} s^{-1} MPa^{-1} (summer) for *A. marina* and 0.57 ± 0.06 kg m^{-1} s^{-1} MPa^{-1} (winter) and 2.93 ± 0.47 kg m^{-1} s^{-1} MPa^{-1} (summer) as a mean for all mangroves]. This difference might be attributed to the actual relative conductivity, which was measured in our study, compared to maximum conductivity reported in the other studies. Also noteworthy is that during the hydraulic conductivity measurements, tree branches originating from high-siltation sites seem to show a higher degree of back-flow. This phenomenon is most likely caused by dehydrated cells craving for water to restore the osmotic gradient and turgor pressure within the cells. This shows that trees in high-siltation sites endured higher stress levels than trees in the low-siltation sites, explaining the slightly lower values in branch hydraulic conductivity.

Responses to siltation in *A. marina*

Trees of *A. marina* responded to buffer any alteration in the hydraulic conductivity, which is linked to tree performance. One of the most striking anatomical adjustments was the tendency towards increased stomatal density (Table 2), a response which has also been reported in other studies using stressed plants (Franks and Beerling 2009; Franks and Farquhar 2001; Hameed and Ashraf 2008; Heckenberger et al. 1998). The combination of smaller stomata and higher

stomatal density results in a better fine regulation of water loss and is positive for the water-use efficiency.

In all sampled *A. marina* trees, a higher phloem band/-growth layer ratio was found in high-siltation sites. This is a common stress adaptation in *A. marina* and other species with successive cambia (Robert et al. 2011). Since siltation causes physiological drought stress and consequently may increase the risk of cavitation, the higher phloem band/growth layer ratio has been related to a mechanism for embolism repair (Salleo et al. 2004, 2006; Zwieniecki et al. 2000).

Responses to siltation in *R. mucronata*

Unlike *A. marina*, *R. mucronata* did not invest in stomatal changes when the soil was silted, with the exception of a declining stomatal area. However, arguable, *R. mucronata* showed tendency towards a slight increase in vessel density under high siltation. This wood anatomical adaptation was previously reported by Schmitz et al. (2006), and attributed to a redundancy strategy to increase conductive safety. This is due to more vessels per cross sectional area creating a higher amount of potential water, nutrient and assimilates transport routes within the tree. As such, a larger proportion of the vessels can remain functional when a fixed number of vessels is embolised (Baas et al. 1983; Mauseth and Plemons Rodriguez 1997; Mauseth and Stevenson 2004; Robert et al. 2009; Villar-Salvador et al. 1997).

Conclusion

Anatomical differences were observed between high- and low-siltation sites. More but smaller leaves with a lowered stomatal area were some of the mutual adaptations of mangrove trees in high-siltation sites. While *A. marina* was directed towards cavitation repair, suggested by the increased phloem band/growth layer ratio, responses in *R. mucronata* were rather directed to avoid cavitation as suggested by the increased vessel density. These anatomical changes together with an unchanged branch hydraulic conductivity point to their role in increasing water-use efficiency. This study highlights the negative impact of siltation on mangrove ecosystems and contributes important information for management programmes for mangrove preservation and rehabilitation and for dredging disposal regulations. While climate change impacts on mangroves are often studied within the context of changed weather patterns, we here indicate that ensuing increase in siltation upon heavy rains (possibly in combination with other and natural events) constitutes a major threat to mangrove health and conservation.

Author contribution statement N.K., N.S. and K.S. supervised the research. J.A.O., N.S. and K.S. designed the study. H.D.D. and J.A.O. collected the samples and data during the field campaign. H.D.D. did the processing of the samples, the analysis and interpretation of the data and wrote the paper. All authors commented on the manuscript.

Acknowledgments The authors are very grateful for the attribution of George Onduso and Eric Okuku, without whom the measurement campaign never would have succeeded. For all the help during the measurement campaign and laboratory work, we would like to thank Samuel Njoroge, Naftali Mukua, Oduor Nancy Awuor, Jan Van Den Bulcke and Piet Dekeyser. Soil analysis was performed by Sturcky Okumu and Oliver Ochola. For statistical support, the authors are grateful towards Rosanna Overholser (FIRE—Fostering Innovative Research based on Evidence—statistical consulting). We also want to thank Veerle De Schepper and Elisabeth M.R. Robert for commenting the M.Sc. text. For logistic support we like to thank Jared Bosire (Kenya Marine and Fisheries Research Institute, KMFRI), Hans Beeckman (Laboratory of Wood Biology and Xylarium, Royal Museum for Central Africa) and Joris Van Acker (Laboratory of Wood Technology—Woodlab, UGent). Additionally, the authors gratefully thank the 3 anonymous reviewers for their constructive comments.

Compliance with ethical standards

Conflict of interest The authors declare that they have no conflict of interest.

References

Abuodha PAW, Kairo JG (2001) Human-induced stresses on mangrove swamps along the Kenyan coast. Hydrobiologia 458:255–265. doi:10.1023/a:1013130916811

Alongi DM (2008) Mangrove forests: resilience, protection from tsunamis, and responses to global climate change. Estuar Coast Shelf Sci 76:1–13. doi:10.1016/j.ecss.2007.08.024

Angeles G, Lopez-Portillo J, Ortega-Escalona F (2002) Functional anatomy of the secondary xylem of roots of the mangrove *Laguncularia racemosa* (L.) Gaertn. (Combretaceae). Trees Struct Funct 16:338–345. doi:10.1007/s00468-002-0171-9

Anyia AO, Herzog H (2004) Water-use efficiency, leaf area and leaf gas exchange of cowpeas under mid-season drought. Eur J Agron 20:327–339. doi:10.1016/s1161-0301(03)00038-8

APHA (1998) Standard method for the examination of water and waste-water. 20th edn. American Public Health Association, Washington, DC

Baas P, Werker E, Fahn A (1983) Some ecological trends in vessel characters. Iawa Bull 4:141–159

Ball MC (1988) Ecophysiology of mangroves. Trees Struct Funct 2:129–142

Brakel W (1982) Tidal patterns on the East African coast and their implications for the littoral biota. In: Proceedings of the symposium on the coastal and marine environment of the Red Sea, Gulf of Aden and tropical Western Indian Ocean, pp 403–418

Brugnoli E, Lauteri M (1991) Effects of salinity on stomatal conductance, photosynthetic capacity, and carbon isotope discrimination of salt-tolerant (*Gossypium hirsutum* L.) and salt-sensitive (*Phaseolus vulgaris* L.) C3 non-halophytes. Plant Physiol 95:628–635. doi:10.1104/pp.95.2.628

Burghardt M, Burghardt A, Gall J, Rosenberger C, Riederer M (2008) Ecophysiological adaptations of water relations of *Teucrium chamaedrys* L. to the hot and dry climate of xeric limestone sites in Franconia (Southern Germany). Flora 203:3–13. doi:10.1016/j.flora.2007.11.003

Carr DJ (2000) On the supposed changes in stomatal frequency and size with height of leaf insertion. Ann Bot 86:911–912. doi:10.1006/anbo.2000.1258

Castañeda-Moya E, Twilley RR, Rivera-Monroy VH, Zhang K, Davis SE III, Ross M (2010) Sediment and nutrient deposition associated with Hurricane Wilma in mangroves of the Florida Coastal Everglades. Estuar Coasts 33:45–58

Choat B et al (2011) Xylem traits mediate a trade-off between resistance to freeze-thaw-induced embolism and photosynthetic capacity in overwintering evergreens. New Phytol 191:996–1005. doi:10.1111/j.1469-8137.2011.03772.x

Ellison JC (1998) Impacts of sediment burial on mangroves. Mar Pollut Bull 37:420–426

Franks PJ, Beerling DJ (2009) Maximum leaf conductance driven by CO_2 effects on stomatal size and density over geologic time. Proc Natl Acad Sci USA 106:10343–10347. doi:10.1073/pnas.0904209106

Franks PJ, Farquhar GD (2001) The effect of exogenous abscisic acid on stomatal development, stomatal mechanics, and leaf gas exchange in *Tradescantia virginiana*. Plant Physiol 125:935–942. doi:10.1104/pp.125.2.935

Franks PJ, Drake PL, Beerling DJ (2009) Plasticity in maximum stomatal conductance constrained by negative correlation between stomatal size and density: an analysis using *Eucalyptus globulus*. Plant Cell Environ 32:1737–1748. doi:10.1111/j.1365-3040.2009.002031.x

Furukawa K, Wolanski E, Mueller H (1997) Currents and sediment transport in mangrove forests. Estuar Coast Shelf Sci 44:301–310. doi:10.1006/ecss.1996.0120

Gartner H, Nievergelt D (2010) The core-microtome: a new tool for surface preparation on cores and time series analysis of varying cell parameters. Dendrochronologia 28:85–92. doi:10.1016/j.dendro.2009.09.002

Gordon DM (1987) Disturbance to mangroves in tropical-arid Western Australia: hypersalinity and restricted tidal exchange as factors leading to mortality/David M. Gordon. Technical series (Western Australia. Environmental Protection Authority); no. 12. Environmental Protection Authority, Perth. Accessed from http://nla.gov.au/nla.cat-vn1827098

Gu MM, Rom CR, Robbins JA, Oosterhuis DM (2007) Effect of water deficit on gas exchange, osmotic solutes, leaf abscission, and growth of four birch genotypes (*Betula* L.) under a controlled environment. HortScience 42:1383–1391

Hameed M, Ashraf M (2008) Physiological and biochemical adaptations of *Cynodon dactylon* (L.) Pers. from the Salt Range (Pakistan) to salinity stress. Flora 203:683–694. doi:10.1016/j.flora.2007.11.005

Hao GY et al (2009) Hydraulic redistribution in dwarf *Rhizophora mangle* trees driven by interstitial soil water salinity gradients: impacts on hydraulic architecture and gas exchange. Tree Physiol 29:697–705. doi:10.1093/treephys/tpp005

Heckenberger U, Roggatz U, Schurr U (1998) Effect of drought stress on the cytological status in *Ricinus communis*. J Exp Bot 49:181–189. doi:10.1093/jexbot/49.319.181

Kathiresan K, Bingham BL (2001) Biology of mangroves and mangrove ecosystems. In: Southward AJ, Tyler PA, Young CM, Fuiman LA (eds) Advances in marine biology, vol 40. Advances in marine biology. pp 81–251. doi:10.1016/s0065-2881(01)40003-4

Krauss KW, Lovelock CE, McKee KL, Lopez-Hoffman L, Ewe SML, Sousa WP (2008) Environmental drivers in mangrove establishment and early development: a review. Aquat Bot 89:105–127. doi:10.1016/j.aquabot.2007.12.014

Lieth H, Berlekamp J, Fuest S, Riediger S (1999) Climate diagrams of the world. CD-series: climate and biosphere. Blackhuys Publishers, Leiden

López-Portillo J, Ewers FW, Angeles G (2005) Sap salinity effects on xylem conductivity in two mangrove species. Plant, Cell Environ 28:1285–1292. doi:10.1111/j.1365-3040.2005.01366.x

Lovelock CE, Ball MC, Choat B, Engelbrecht BMJ, Holbrook NM, Feller IC (2006) Linking physiological processes with mangrove forest structure: phosphorus deficiency limits canopy development, hydraulic conductivity and photosynthetic carbon gain in dwarf *Rhizophora mangle*. Plant, Cell Environ 29:793–802. doi:10.1111/j.1365-3040.2005.01446.x

Lugo AE, Cintron G (1975) The mangrove forests of Puerto Rico and their management. In: Proceedings of the international symposium on biology and management of mangroves, Gainesville, University of Florida

Mauseth JD, Plemons Rodriguez BJ (1997) Presence of paratracheal water storage tissue does not alter vessel characters in cactus wood. Am J Bot 84:815–822. doi:10.2307/2445817

Mauseth JD, Stevenson JF (2004) Theoretical considerations of vessel diameter and conductive safety in populations of vessels. Int J Plant Sci 165:359–368. doi:10.1086/382808

McClenahan K, Macinnis-Ng C, Eamus D (2004) Hydraulic architecture and water relations of several species at diverse sites around Sydney. Aust J Bot 52:509–518. doi:10.1071/bt03123

McKee KL (1996) Growth and physiological responses of neotropical mangrove seedlings to root zone hypoxia. Tree Physiol 16:883–889

Mohamed MOS, Neukermans G, Kairo JG, Dahdouh-Guebas F, Koedam N (2009) Mangrove forests in a peri-urban setting: the case of Mombasa (Kenya). Wetlands Ecol Manage 17:243–255. doi:10.1007/s11273-008-9104-8

Naz N, Hameed M, Ashraf M, Al-Qurainy F, Arshad M (2010) Relationships between gas-exchange characteristics and stomatal structural modifications in some desert grasses under high salinity. Photosynthetica 48:446–456. doi:10.1007/s11099-010-0059-7

Okello JA, Robert EMR, Beeckman H, Kairo JG, Dahdouh-Guebas F, Koedam N (2014) Effects of experimental sedimentation on the phenological dynamics and leaf traits of replanted mangroves at Gazi Bay. Ecol Evol, Kenya. doi:10.1002/ece3.1154

Ounis A, Cerovic Z, Briantais J, Moya I (2005) Rasband WS, Image J. US National Institutes of Health, Bethesda

Parson TR, Maita Y, Lalli CM (1984) A manual of chemical and biological methods for seawater analysis. Pergamon Press, Oxford

Pi N, Tam N, Wu Y, Wong M (2009) Root anatomy and spatial pattern of radial oxygen loss of eight true mangrove species. Aquat Bot 90:222–230

Quarrie SA, Jones HG (1977) Effects of abscisic-acid and water stress on development and morphology of wheat. J Exp Bot 28:192. doi:10.1093/jxb/28.1.192

Quisthoudt K, Adams J, Rajkaran A, Dahdouh-Guebas F, Koedam N, Randin CF (2013) Disentangling the effects of global climate and regional land-use change on the current and future distribution of mangroves in South Africa. Biodivers Conserv 22:1369–1390. doi:10.1007/s10531-013-0478-4

Robert EMR, Koedam N, Beeckman H, Schmitz N (2009) A safe hydraulic architecture as wood anatomical explanation for the difference in distribution of the mangroves Avicennia and Rhizophora. Funct Ecol 23:649–657. doi:10.1111/j.1365-2435.2009.01551.x

Robert EMR et al (2011) Successive cambia: a developmental oddity or an adaptive structure? PLoS ONE. doi:10.1371/journal.pone.0016558

Salleo S, Lo Gullo MA, Trifilo P, Nardini A (2004) New evidence for a role of vessel-associated cells and phloem in the rapid xylem refilling of cavitated stems of *Laurus nobilis* L. Plant, Cell Environ 27:1065–1076. doi:10.1111/j.1365-3040.2004.01211.x

Salleo S, Trifilo P, Lo Gullo MA (2006) Phloem as a possible major determinant of rapid cavitation reversal in stems of *Laurus nobilis* (laurel). Funct Plant Biol 33:1063–1074. doi:10.1071/fp06149

Schmitz N, Verheyden A, Beeckman H, Kairo JG, Koedam N (2006) Influence of a salinity gradient on the vessel characters of the mangrove species *Rhizophora mucronata*. Ann Bot 98:1321–1330. doi:10.1093/aob/mcl224

Schmitz N, Jansen S, Verheyden A, Kairo JG, Beeckman H, Koedam N (2007) Comparative anatomy of intervessel pits in two mangrove species growing along a natural salinity gradient in Gazi Bay, Kenya. Ann Bot 100:271–281. doi:10.1093/aob/mcm103

Schmitz N, Robert EMR, Verheyden A, Kairo JG, Beeckman H, Koedam N (2008) A patchy growth via successive and simultaneous cambia: key to success of the most widespread mangrove species *Avicennia marina*? Ann Bot 101:49–58. doi:10.1093/aob/mcm280

Scholander PF, Hemmingsen EA, Hammel HT, Bradstreet EDP (1964) Hydrostatic pressure and osmotic potential in leaves of mangroves and some other plants. Proc Natl Acad Sci USA 52:119. doi:10.1073/pnas.52.1.119

Schurr U, Heckenberger U, Herdel K, Walter A, Feil R (2000) Leaf development in *Ricinus communis* during drought stress: dynamics of growth processes, of cellular structure and of sink-source transition. J Exp Bot 51:1515–1529. doi:10.1093/jexbot/51.350.1515

Sperry JS, Donnelly JR, Tyree MT (1988) A method for measuring hydraulic conductivity and embolism in xylem. Plant, Cell Environ 11:35–40. doi:10.1111/j.1365-3040.1988.tb01774.x

Stuart SA, Choat B, Martin KC, Holbrook NM, Ball MC (2007) The role of freezing in setting the latitudinal limits of mangrove forests. New Phytol 173:576–583. doi:10.1111/j.1469-8137.2006.01938.x

Terrados J et al (1997) The effect of increased sediment Accretion on the survival and growth of *Rhizophora apiculata* seedlings. Estuar Coast Shelf Sci 45:697–701. doi:10.1006/ecss.1997.0262

Thomas L (1997) Retrospective power analysis. Conserv Biol 11:276–280

Tomlinson PB (1986) The botany of mangroves. University Press, Cambridge

Vaiphasa C, De Boer WF, Panitchart S, Vaiphasa T, Bamrongrugsa N, Santitamnont P (2007) Impact of solid shrimp pond waste materials on mangrove growth and mortality: a case study from Pak Phanang, Thailand. Hydrobiologia 591:47–57. doi:10.1007/s10750-007-0783-6

van Mensvoort T (1998) Mangrove research discussion list. Communication

Villar-Salvador P, Castro-Diez P, Perez-Rontome C, Montserrat-Martí G (1997) Stem xylem features in three Quercus (Fagaceae) species along a climatic gradient in NE Spain. Trees Struct Funct 12:90–96. doi:10.1007/pl00009701

Zwieniecki MA, Hutyra L, Thompson MV, Holbrook NM (2000) Dynamic changes in petiole specific conductivity in red maple (*Acer rubrum* L.), tulip tree (*Liriodendron tulipifera* L.) and northern fox grape (*Vitis labrusca* L.). Plant, Cell Environ 23:407–414. doi:10.1046/j.1365-3040.2000.00554.x